SOIL-WATER CHARACTERISTIC CURVES AND DUAL POROSITY OF SAND–DIATOMACEOUS EARTH MIXTURES

By Craig A. Burger[1] and Charles D. Shackelford,[2] Associate Member, ASCE

ABSTRACT: The soil-water characteristic curves (SWCCs) for sand–pelletized diatomaceous earth mixtures are measured. The measured SWCCs are bimodal due to two distinct pore-size distributions associated with the microscopic (intrapellet) and macroscopic (interpellet) porosity regions of the pelletized diatomaceous earth. The measured data for the bimodal SWCCs are fit with modified forms of the Brooks-Corey, van Genuchten, and Fredlund-Xing SWCC functions, and the microscopic and macroscopic porosity portions of the mixtures are determined from the SWCC fits. Both the total and the microscopic porosity of the mixtures increase with increased percentage by dry weight of diatomaceous earth in the mixtures. However, the macroscopic porosity of the mixtures is essentially independent of the diatomaceous earth content due to the similarity in the particle-size distributions of the sand and the diatomaceous earth. The results suggest that sand–diatomaceous earth mixtures may be useful in applications where an increase in water-holding capacity (that is, relative to sand) is desired, such as in landfill covers. In such applications, a balance between the increase in cost and the increase in water-holding capacity due to the use of the diatomaceous earth must be achieved.

INTRODUCTION

Natural diatomaceous earth, or diatomite, is a sedimentary deposit formed from the inorganic skeletal remains of single-cell algae and plankton. The shells resulting from the decay of these skeletal remains form a deposit with interconnected pores of sizes appropriate for microbiological growth and filtering of solids suspended in water. The structure and distribution of these interconnected pores results in a relatively high porosity (typically >70%) and high surface area (Breese 1994). Naturally occurring diatomaceous earth has been used as engineered fill in California (Capik and Khilnani 1989; Day 1995), and the natural deposits of diatomaceous earth also are mined and processed to segregate the particles by size and remove impurities for commercial use. The processing of natural diatomaceous earth results in the formation of particle sizes that range from powder to pellets several millimeters in diameter [for example, Burger and Shackelford (2001)].

In the case of aggregated diatomaceous earth, two distinct pore-size distributions commonly exist, one for the macroscopic porosity region between the particles, and another for the microscopic porosity region within the particles. The existence of two distinct pore-size distributions in soils results in bimodal soil behavior. For example, Stoicescu et al. (1998) measured double-humped shaped or bimodal soil-water characteristic curves for sand-bentonite mixtures consisting of a relatively uniform sand mixed with 8% (by dry weight) of bentonite. Stoicescu et al. (1998) attributed the bimodal shape of the soil-water characteristic curve to pore water trapped between both the larger, interaggregate pores between the sand particles and bentonite platelets and the smaller, intra-aggregate pores entirely within the oriented bentonite platelets. More recently, Fredlund et al. (2000) have proposed the use of a bimodal mathematical function to describe the grain-size curve of gap-graded soils containing two distinct grain-size distributions (and therefore two distinct pore-size distributions). Fredlund et al. (2000) note that their proposed mathematical function for the grain-size curve provides a basis for the eventual estimation of the soil-water characteristic curve of a soil.

Burger and Shackelford (2001) measured bimodal soil-water characteristic curves for diatomaceous earth specimens consisting of uniform, coarse-grained pellets with nominal diameters of either 1 or 2 mm, corresponding to total porosities at maximum dry density of 0.764 and 0.725, respectively. The bimodal shapes of the soil-water characteristic curves were attributed to the existence of both a macroscopic (interpellet) and a microscopic (intrapellet) porosity. The bimodal soil-water characteristic curves also proved useful in estimating the percentage of the total porosity attributable to the microscopic porosity, which ranged from 45.0 to 47.9% of the total porosities for the two diatomaceous earth materials.

The relatively high total porosity and dual porosity nature of pelletized diatomaceous earth observed by Burger and Shackelford (2001) make pelletized diatomaceous earth a potentially ideal material for several applications in waste disposal systems (for example, landfills). Examples of these applications include uses as (1) a moisture (capillary) barrier in landfill covers; (2) a soil amendment to enhance water retention, drainage, and vegetative cover growth in landfill covers or soils with poor water retention or runoff characteristics; and (3) a biological growth medium for in situ leachate treatment in landfill liner systems. However, the cost associated with the sole use of pelletized diatomaceous earth in these applications may be prohibitive. For example, the cost of bulk quantities of the pelletized diatomaceous earth used in this study ranged from $66 to $78 per 45 kg (100 lb) of material. As a result, mixtures of pelletized diatomaceous earth and less expensive fill materials, such as sand, are more economical.

Since many of the potential applications of sand–diatomaceous earth mixtures in waste disposal systems involve consideration of unsaturated liquid flow, a knowledge of the soil-water characteristic curves of these mixtures is required. Also, the water-holding capacity associated with the dual porosity nature of sand–diatomaceous earth mixtures should depend, in part, on the amount of pelletized diatomaceous earth in the mixture. Thus, the overall objective of this study is to extend the previous study of Burger and Shackelford (2001) by evaluating the influence of the content of pelletized diatomaceous earth on the soil-water characteristic curves and the resulting dual porosity of sand–diatomaceous earth mixtures. The objective will be accomplished by measuring the soil-water characteristic curves of sand–diatomaceous earth mixtures using several different methods of measurement to cover a broad range of soil suctions. In addition, the measured data will be

[1]Assoc. Engr., Montgomery Watson Mining Group, 165 South Union Blvd., Ste. 410, Lakewood, CO 80228; formerly, Grad. Student, Dept. of Civ. Engrg., Colo. State Univ., Fort Collins, CO 80523-1372.

[2]Prof., Dept. of Civ. Engrg., Colo. State Univ., Fort Collins, CO 80523-1372 (corresponding author). E-mail: shackel@engr.colostate.edu

Note. Discussion open until February 1, 2002. To extend the closing date one month, a written request must be filed with the ASCE Manager of Journals. The manuscript for this paper was submitted for review and possible publication on October 17, 2000; revised April 16, 2001. This paper is part of the ***Journal of Geotechnical and Geoenvironmental Engineering***, Vol. 127, No. 9, September, 2001. ©ASCE, ISSN 1090-0241/01/0009-0790–0800/$8.00 + $.50 per page. Paper No. 22549.

analyzed using several soil-water characteristic curve functions, and the amount of pore space that can be attributed to the microscopic and macroscopic porosity regions of the sand–diatomaceous earth mixtures will be determined from functional fits to the measured soil-water characteristic curves.

MATERIALS AND EXPERIMENTAL METHODS

Materials

The constituent materials used in this study represent two sizes of processed diatomaceous earth pellets and two sands with different particle-size distributions. The diatomaceous earth pellets are the same materials previously studied by Burger and Shackelford (2001) and are known commercially as Isolite (Sundine Enterprises, Inc., Denver, Colo.) under the product names CG1 and CG2, corresponding to average pellet diameters of approximately 1 and 2 mm, respectively. The two sands used in this study are referred to as 20-60 and 10-20 sands because 90% by weight of the 20-60 and 10-20 sands are retained between the No. 20 and No. 60, and the No. 10 and No. 20 sieves, respectively. Fig. 1 is a photograph of the CG1 and CG2 pellets and the two sands, and Fig. 2 shows the particle-size distributions (ASTM D 422) for the constituent materials.

As shown in Fig. 2, all of the materials are uniformly graded. The 20-60 sand is finer than both the 10-20 sand and the CG1 and CG2 pellets. The 10-20 sand is coarser than the CG1 pellets and finer than the CG2 pellets. Both of the sands as well as the CG1 and CG2 pellets classify as poorly graded sands, according to ASTM D 2487.

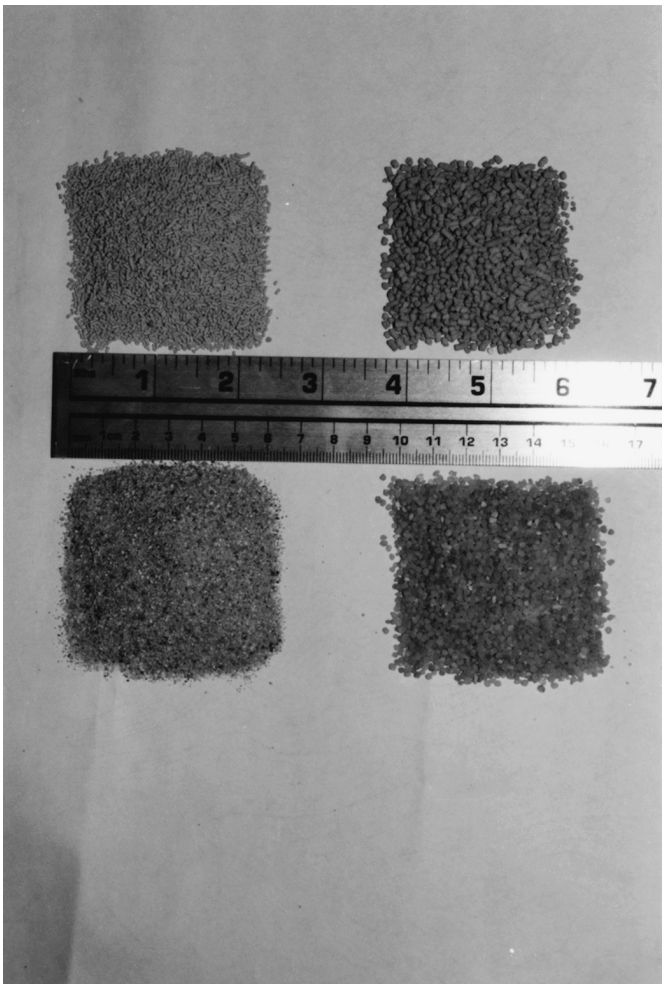

FIG. 1. Photograph of Constituent Materials Used in Sand–Diatomaceous Earth (DE) Mixtures: CG1 DE (Top Left); CG2 DE (Top Right); 20-60 Sand (Bottom Left); 10-20 Sand (Bottom Right)

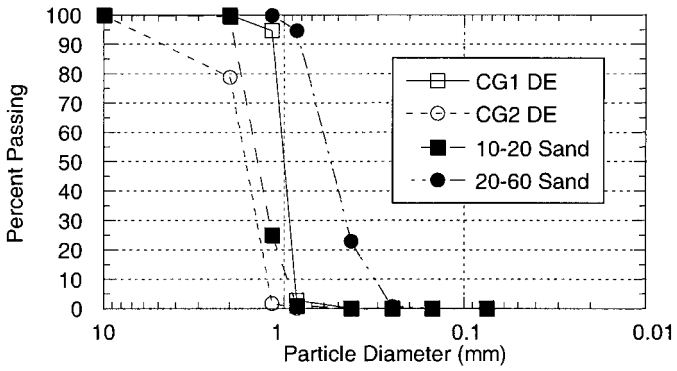

FIG. 2. Particle-Size Distributions for Sands and Diatomaceous Earth (DE) Constituent Materials

TABLE 1. Physical Properties of Constituent Materials

Property	ASTM standard	Type of Diatomaceous Earth		Type of Sand	
		CG1	CG2	20-60	10-20
Specific gravity of solids, G_s	D 854	2.28	2.24	2.65	2.65
Maximum dry density, $\rho_{d,max}$ (g/cm^3)	D 4253	0.537	0.617	1.39	1.66
Minimum total porosity, $n_{T,min}$ (%)[a]	NA	76.4	72.5	47.5	37.2
Minimum dry density, $\rho_{d,min}$ (g/cm^3)	D 4254	0.506	0.584	1.26	1.54
Maximum total porosity, $n_{T,max}$ (%)[a]	NA	77.8	73.9	52.4	41.9

[a] $n_{T,min} = 1 - \rho_{d,max}/G_s\rho_w$, $n_{T,max} = 1 - \rho_{d,min}/G_s\rho_w$, where ρ_w = density of water.

The primary difference between the sands and the CG1 and CG2 pellets is the existence of a microscopic porosity within the CG1 and CG2 pellets (Burger and Shackelford 2001). Thus, a packing of the pellets will consist of both a macroscopic porosity between the pellets (interpellet porosity) and a microscopic porosity within the pellets (intrapellet porosity). This microscopic porosity typically accounts for approximately 50% of the total porosity, depending on the relative densities and sizes of the pellets (Burger and Shackelford 2001).

The measured specific gravity (ASTM D 854) and the maximum and minimum densities (ASTM D 4253 and D 4254, respectively) for each material are shown in Table 1, along with the calculated total porosity at the maximum and minimum densities. The lower dry densities for the CG1 and CG2 pellets reflect the existence of internal pore space in the pellets. The total porosity of the CG1 and CG2 pellets also ranges from about 25 to 40 percentage points higher than the total porosity of the sands. The total porosity of the 10-20 sand is approximately 10 percentage points lower than the total porosity of the 20-60 sand due to the slightly larger particle sizes of the 10-20 sand.

Mixtures

In this study, soil-water characteristic curves are measured for 12 different mixtures of the two sands and the CG1 and CG2 pellets. Mixtures of CG1 pellets with the 20-60 sand, GC2 pellets with the 20-60 sand, and CG2 pellets with the 10-20 sand were prepared at four different percentages of diatomaceous earth, ranging from 4 to 30% by dry weight. The

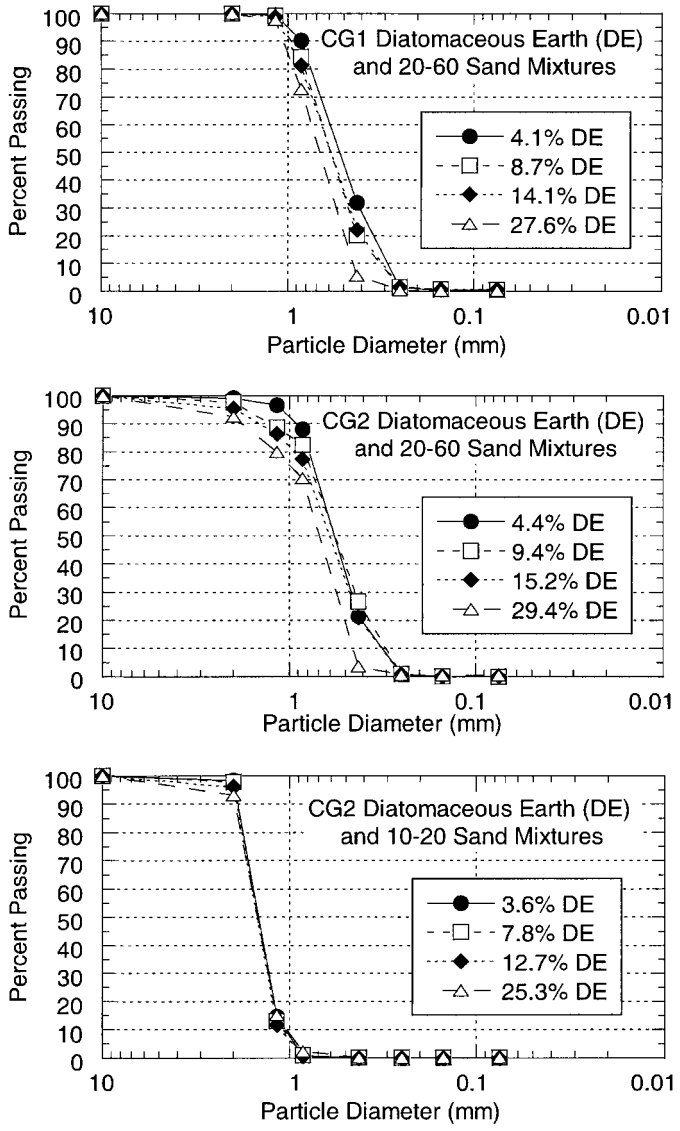

FIG. 3. Particle-Size Distributions for Sand–Diatomaceous Earth Mixtures

mechanical particle-size distributions (ASTM D 422) for all the mixtures also are shown in Fig. 3.

The measured specific gravity and the maximum and minimum densities of the mixtures are given in Table 2, along with total porosity values calculated at the maximum and minimum densities. The total porosities of the mixtures are all greater than those for the constituent sand and increase with increasing diatomaceous earth content. This increase in total porosity with increasing diatomaceous earth content is consistent with an increase in the contribution of the microscopic (intrapellet) porosity associated with the pelletized diatomaceous earth.

Measurement of Soil-Water Characteristic Curves

Three methods were used to measure the soil-water characteristic curve data of the sand–diatomaceous earth mixtures reported in this study: (1) the Tempe cell method, (2) the pressure plate method, and (3) the filter paper method. The use of these three methods was based primarily on two considerations: (1) the need to measure soil-water characteristic curve data over a wide range of soil suctions; and (2) the desire to measure the soil-water characteristic curve data within a reasonable period ($\leq$8 days). Soil suctions $\leq$3.4 kPa were measured using Tempe cells (model No. 1400, Soil Moisture Co., Santa Barbara, Calif.); volumetric water contents corresponding to soil suctions ranging from 3.4 to 100 kPa were measured using a pressure plate apparatus (model No. 1600, Soil Moisture Co., Santa Barbara, Calif.) and the procedures described in ASTM D 2325; and soil suctions greater than 196 kPa were obtained using the filter paper method. No soil-water characteristic curve data were measured for soil suctions between 100 and 196 kPa in this study. Further details regarding the soil suction measurements are provided by Burger and Shackelford (2001).

TABLE 2. Physical Properties of Mixtures of Sand and Diatomaceous Earth (DE)

Mixture constituents	Percent DE (dry weight)	PHYSICAL PROPERTY				
			Dry Density (g/cm^3)		Total Porosity (%)[d]	
		G_s[a]	$\rho_{d,max}$[b]	$\rho_{d,min}$[c]	$n_{T,min}$	$n_{T,max}$
CG1 and 20-60 sand	4.1	2.64	1.381	1.227	47.7	53.5
	8.7	2.61	1.298	1.142	50.3	56.2
	14.1	2.59	1.204	1.064	53.5	58.9
	27.6	2.53	0.996	0.897	60.6	64.6
CG2 and 20-60 sand	4.4	2.63	1.388	1.229	47.2	53.3
	9.4	2.60	1.324	1.164	49.1	55.2
	15.2	2.58	1.243	1.090	51.8	57.7
	29.4	2.52	1.082	0.974	57.1	61.3
CG2 and 10-20 sand	3.6	2.63	1.562	1.451	40.6	44.8
	7.8	2.60	1.479	1.364	43.1	47.5
	12.7	2.59	1.351	1.272	47.8	50.9
	25.3	2.53	1.152	1.073	54.5	57.6

[a]ASTM D 854.
[b]ASTM D 4253.
[c]ASTM D 4254.
[d]$n_{T,min} = 1 - \rho_{d,max}/G_s\rho_w$, $n_{T,max} = 1 - \rho_{d,min}/G_s\rho_w$, where ρ_w = density of water.

Specimen Preparation

Soil suction measurements were performed for specimens prepared at the maximum dry density (ASTM D 4253) to reduce the effect of changes in density on the size of the macroscopic pores. The dimensions of the specimen container were measured using a micrometer, and the volumes of the specimen containers were calculated from these measurements. The mass of dry material based on the maximum dry density was calculated using the volumes of the specimen containers.

For the Tempe cell and pressure plate measurements, the dry mass of material corresponding to the maximum dry density was placed directly into the specimen rings and saturated through the porous plate in accordance with ASTM D 2325. For the filter paper measurements, the amount of dry material corresponding to the product of the maximum dry density and the volume of the specimen containers was weighed. The resulting material was washed with deionized water (DIW) to remove soluble salts, saturated by immersion in DIW for 24 h, and air-dried until the desired water content was achieved. After completion of air-drying, the material was placed in the specimen containers at the maximum dry density.

SOIL-WATER CHARACTERISTIC CURVE FUNCTIONS

Unimodal Functions

Three unimodal soil-water characteristic curve functions were considered for use in this study: (1) the Brooks-Corey function (Brooks and Corey 1964); (2) the van Genuchten function (van Genuchten 1980); and (3) the Fredlund-Xing function (Fredlund and Xing 1994). The Brooks-Corey and van Genuchten functions were considered because they com-

TABLE 3. Unimodal Soil-Water Characteristic Curve Functions Used in Study

Name	Form[a]	Reference
Brooks-Corey	$\theta = \begin{cases} \theta_r + (\theta_s - \theta_r)\left(\frac{\psi}{\psi_d}\right)^{-\lambda}; & \psi_d < \psi \\ \theta_s; & \psi \le \psi_d \end{cases}$	Brooks and Corey (1964)
van Genuchten	$\theta = \theta_r + (\theta_s - \theta_r)\left[\frac{1}{1 + (\alpha\psi)^{\beta}}\right]^{1-1/\beta}$	van Genuchten (1984)
Fredlund-Xing	$\theta = C(\psi)\frac{\theta_s}{\left\{\ln\left[e + \left(\frac{\psi}{a}\right)^n\right]\right\}^m}$ where $C(\psi)$ = correcting function given by $C(\psi) = 1 - \frac{\ln\left(1 + \frac{\psi}{\psi_r}\right)}{\ln\left(1 + \frac{10^6}{\psi_r}\right)}$	Fredlund and Xing (1994)

[a]θ = volumetric water content; θ_r = residual volumetric water content; θ_s = saturated volumetric water content; ψ = soil suction; ψ_d = air entry or displacement suction; ψ_r = soil suction corresponding to θ_r; e = base of natural logarithm; λ (pore size distribution index), α, β, a, m, n = fitting parameters.

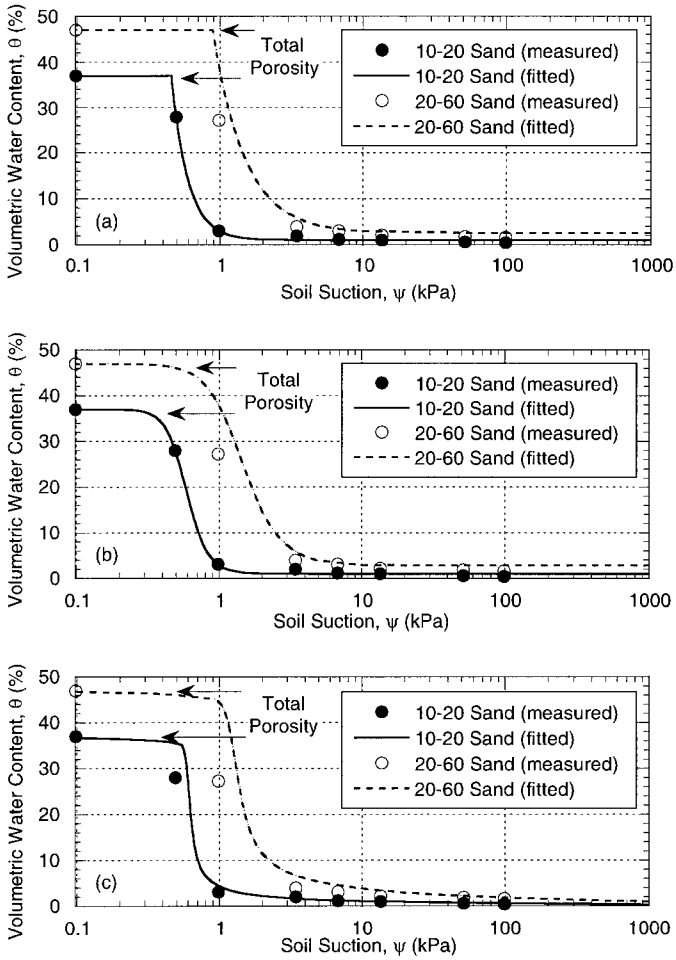

FIG. 4. Measured and Fitted Soil-Water Characteristic Curves for 10-20 and 20-60 Sands Using (a) Brooks-Corey, (b) van Genuchten, and (c) Fredlund-Xing Unimodal Curve Fitting Functions

TABLE 4. Bimodal Soil-Water Characteristic Curve Functions Used in Study (from Burger and Shackelford 2001)

Name	Form[a]
Brooks-Corey	$\theta = \begin{cases} \theta_r + (\theta_j - \theta_r)\left(\frac{\psi}{\psi'_d}\right)^{-\lambda'}; & \psi_j < \psi \\ \theta_j + (\theta_s - \theta_j)\left(\frac{\psi}{\psi_d}\right)^{-\lambda}; & \psi_d < \psi \le \psi_j \\ \theta_s; & \psi \le \psi_d \end{cases}$
van Genuchten	$\theta = \begin{cases} \theta_r + (\theta_j - \theta_r)\left[\frac{1}{1 + (\alpha'\psi)^{\beta'}}\right]^{(1-1/\beta')}; & \psi_j < \psi \\ \theta_j + (\theta_s - \theta_j)\left[\frac{1}{1 + (\alpha\psi)^{\beta}}\right]^{(1-1/\beta)}; & \psi \le \psi_j \end{cases}$
Fredlund-Xing	$\theta = \begin{cases} C(\psi) = \frac{\theta_j}{\left\{\ln\left[e + \left(\frac{\psi}{a'}\right)^{n'}\right]\right\}^{m'}}; & \psi_j < \psi \\ C(\psi)\frac{\theta_s}{\left\{\ln\left[e + \left(\frac{\psi}{a}\right)^{n}\right]\right\}^{m}}; & \psi \le \psi_j \end{cases}$ where $C(\psi)$ = correcting function given by $C(\psi) = \begin{cases} 1 - \frac{\ln\left[1 + \left(\frac{\psi}{\psi'_r}\right)\right]}{\ln\left[1 + \left(\frac{10^6}{\psi'_r}\right)\right]}; & \psi_j < \psi \\ 1 - \frac{\ln\left[1 + \left(\frac{\psi}{\psi_r}\right)\right]}{\ln\left[1 + \left(\frac{10^6}{\psi_r}\right)\right]}; & \psi \le \psi_j \end{cases}$

[a]θ = volumetric water content; θ_j = junction volumetric water content; θ_r = residual volumetric water content; θ_s = saturated volumetric water content; ψ = soil suction; ψ_j = junction soil suction; ψ_d, ψ'_d = air-entry or displacement suctions for macroscopic, microscopic portions of data; ψ_r, ψ'_r = residual soil suctions for macroscopic, microscopic portions of data; e = base of natural logarithm; λ, α, β, a, m, n = fitting parameters for macroscopic portion of data; λ', α', β', a', m', n' = fitting parameters for microscopic portion of data.

TABLE 5. Soil-Water Characteristic Curve-Fit Parameters for Sands Used in Sand–Diatomaceous Earth Mixtures

Soil-water characteristic curve function[a]	Fitting parameter[a]	Type of Sand	
		20-60	10-20
Brooks-Corey (1964)	θ_r (%)	2.6	1.0
	θ_s (%)	47.0	37.0
	ψ_d (m)	0.09	0.05
	λ	1.93	3.73
	R^2	0.999	0.999
van Genuchten (1984)	θ_r (%)	2.7	1.0
	θ_s (%)	47.0	37.0
	α	7.56	17.3
	β	3.69	6.20
	R^2[b]	0.999	0.999
Fredlund-Xing (1994)	θ_r (%)	3.7	1.1
	θ_s (%)	47.0	37.0
	a (kPa)	1.01	0.50
	n	12.79	31.49
	m	0.72	0.75
	ψ_r	1.61	0.67
	Error[c]	<0.01	<0.01

[a]See Table 3.
[b]R^2 = coefficient of determination.
[c]Error = sum of squared residuals.

monly are used in simulating unsaturated liquid flow through porous media. The Fredlund-Xing function also was considered because it reportedly provides a better description of the soil-water characteristic curve over a wide range of suctions (Leong and Rahardjo 1997). The forms of these unimodal soil-water characteristic curve functions are given in Table 3.

Bimodal Functions

The method used in this study to fit the measured bimodal soil-water characteristic curve data using the unimodal Brooks-Corey, van Genuchten, and Fredlund-Xing functions follows the procedure developed by Smettem and Kirby (1990), as described by Burger and Shackelford (2001). In this method, a suction value, ψ_j, and corresponding volumetric water content, θ_j, are selected at the junction where the macroscopic porosity appears to have been completely desaturated, and the microscopic porosity begins to desaturate. The data for suctions greater or less than ψ_j are fit separately, using the unimodal forms of the soil-water characteristic curve functions for each set of data producing two sets of fitting parameters. This method is similar to that proposed by Fredlund et al. (2000) for describing the grain-size curve of a gap-graded (bimodal) soil, in that the procedure essentially consists of superimposing two unimodal functions to cover the full range of data.

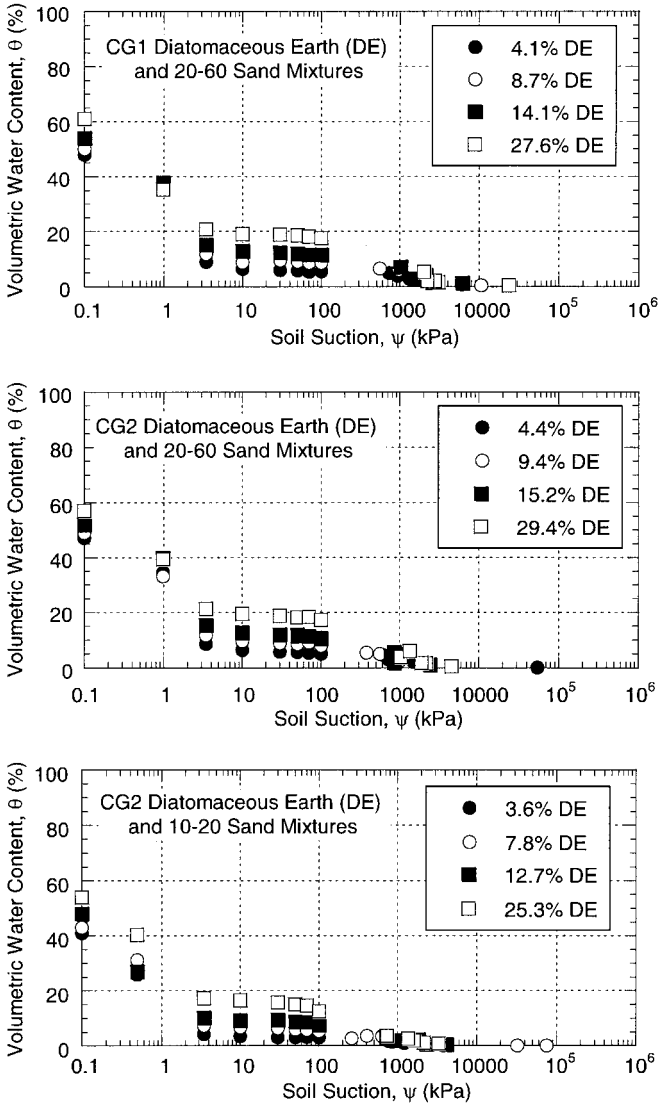

FIG. 5. Measured Soil-Water Characteristic Curve Data for Sand–Diatomaceous Earth Mixtures

The forms of the bimodal soil-water characteristic curve functions used to fit the measured data for suctions greater than ψ_j (that is, microscopic data) and less that ψ_j (that is, macroscopic data) are shown in Table 4. Further details regarding the procedure used to fit the measured soil-water characteristic curve data with bimodal soil-water characteristic curve functions, including a schematic bimodal soil-water characteristic curve illustrating the junction point (ψ_j, θ_j), are given by Burger and Shackelford (2001).

In this study, the RETC code (van Genuchten et al. 1991) was used to fit the Brooks-Corey and van Genuchten functions, and the SoilVision software package (SoilVision Systems Ltd., Saskatoon, Saskatchewan, Canada) was used to fit the Fredlund-Xing function. For the RETC code, the θ_r value from the fit of data less than ψ_j is equal to θ_j. For the SoilVision software used for fitting the Fredlund-Xing function, θ_r was not equal to θ_j since the Fredlund-Xing function forces the water content to be zero at a suction of 10^6 MPa.

RESULTS

Soil-Water Characteristic Curves

Sands

The soil-water characteristic curve data fit with the unimodal Brooks-Corey, van Genuchten, and Fredlund-Xing func-

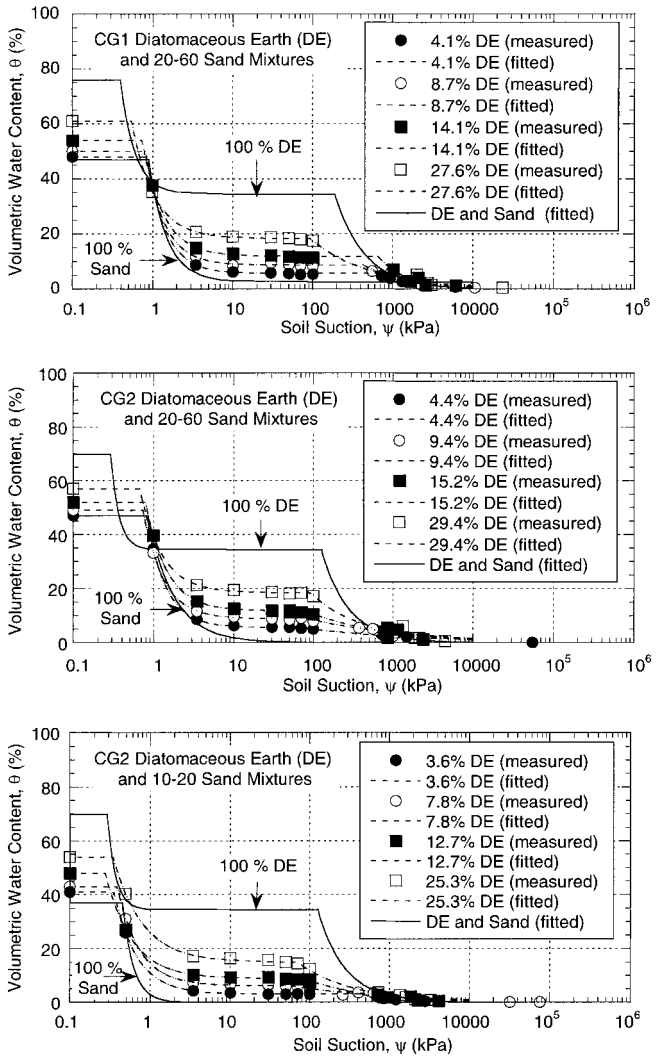

FIG. 6. Fitted Soil-Water Characteristic Curves for Sand–Diatomaceous Earth Mixtures Based on Bimodal Brooks-Corey Fitting Function (100% DE Curve Fits from Burger and Shackelford 2001)

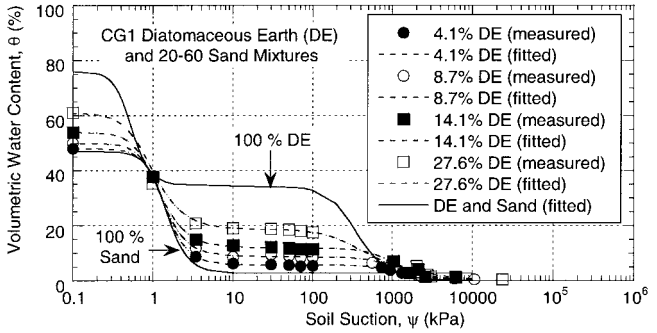

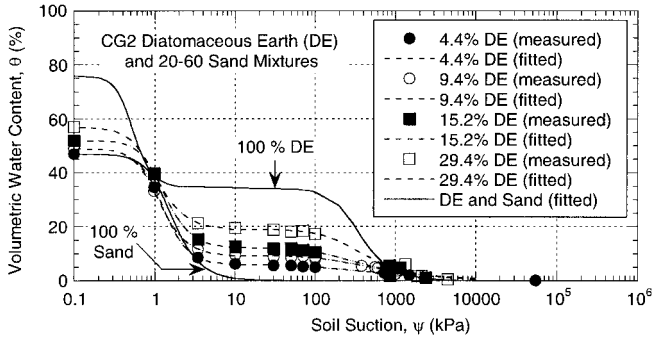

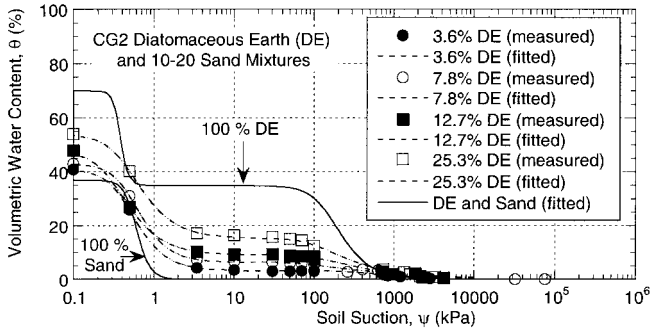

FIG. 7. Fitted Soil-Water Characteristic Curve for Sand–Diatomaceous Earth Mixtures Based on Bimodal van Genuchten Fitting Function (100% DE Curve Fits from Burger and Shackelford 2001)

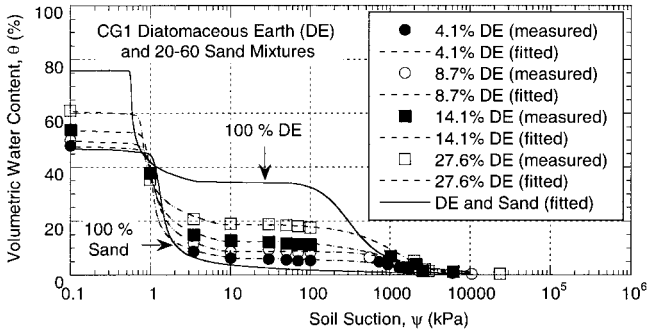

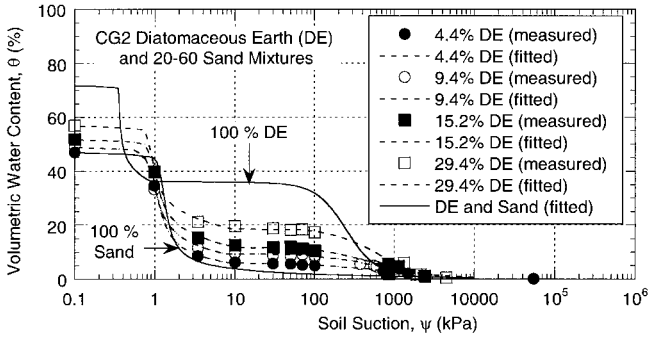

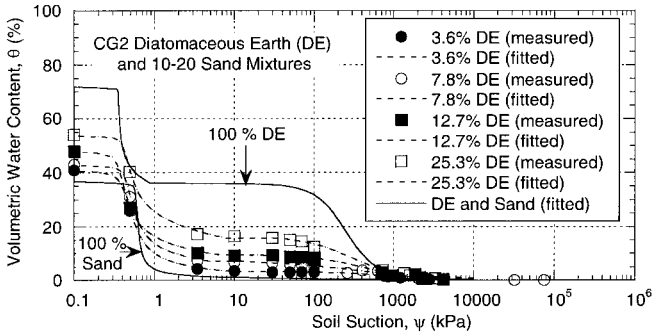

FIG. 8. Fitted Soil-Water Characteristic Curves for Sand–Diatomaceous Earth Mixtures Based on Bimodal Fredlund-Xing Fitting Function (100% DE Curve Fits from Burger and Shackelford 2001)

TABLE 6. Brooks-Corey Bimodal Curve-Fit Parameters for Mixtures of Sand (20-60 and 10-20) and Diatomaceous Earth (CG1 and CG2)[a]

		Macroporosity Portion					Microporosity Portion				
Mixture	DE[b] (%)	θ_j (%)	θ_s (%)	ψ_d (kPa)	λ	R^{2c}	θ_r (%)	θ_j (%)	ψ_d' (kPa)	λ'	R^{2c}
CG1 and 20-60 sand	4.1	5.7	48.0	0.88	1.840	0.99	0.0	5.7	614	0.925	0.98
	8.7	8.8	50.0	0.79	1.820	0.99	0.0	8.8	427	0.789	0.96
	14.1	12.0	54.0	0.69	1.650	0.99	0.0	12.0	655	1.207	0.98
	27.6	18.5	61.0	0.59	1.560	0.99	0.0	18.5	91.0	0.578	0.99
CG2 and 20-60 sand	4.4	5.6	47.0	0.79	1.800	0.99	0.0	5.6	57.1	0.316	0.98
	9.4	9.0	49.0	0.69	1.700	0.99	0.0	9.0	81.8	0.355	0.95
	15.2	11.8	52.0	0.79	1.610	0.99	0.0	11.8	79.2	0.467	0.94
	29.4	18.6	57.0	0.69	1.565	0.99	0.0	18.6	88.5	0.629	0.98
CG2 and 10-20 sand	3.6	3.2	41.0	0.39	1.505	0.99	0.0	3.2	409	1.104	0.98
	7.8	6.4	43.0	0.39	1.550	0.99	0.0	6.4	45.7	0.343	0.96
	12.7	9.0	48.0	0.29	1.290	0.99	0.0	9.0	82.5	0.582	0.98
	25.3	15.2	54.0	0.29	1.190	0.99	0.0	15.2	65.9	0.641	0.99

[a]See Table 4.
[b]% DE = percentage of diatomaceous earth by dry weight in mixture.
[c]R^2 = coefficient of determination for curve fit.

tions for the 20-60 and 10-20 sands is shown in Fig. 4. The soil-water characteristic curves for the sand are typical of coarse-grained materials with unimodal soil-water characteristic curves. The curve fit parameters for the 20-60 and 10-20 sands for the Brooks-Corey, van Genuchten, and Fredlund-Xing functions are listed in Table 5. In performing the curve fits, the saturated volumetric water content was assumed to be equal to the total porosity (that is, $\theta_s = n_T$), since the measurement of the drying soil-water characteristic curve was performed on initially saturated samples.

Sand-Diatomaceous Earth Mixtures

The measured soil-water characteristic curve data for all sand–diatomaceous earth mixtures are shown in Fig. 5. For all mixtures, the data indicate that an asymptotic value for the volumetric water content, θ, is approached as the mixture is dried from saturation to soil suctions ranging from ~10 to 100 kPa, and that subsequent drying reduces θ to a value approaching zero at soil suctions ranging from ~1,000 to 100,000 kPa. This trend in the measured soil-water characteristic curve data is more evident for the mixtures containing the higher contents of the diatomaceous earth, and is consistent with bimodal soil behavior as expected on the basis of the dual porosity nature of the pelletized diatomaceous earth. Thus, in contrast to the soil-water characteristic curve data for the sand (Fig. 4), a unimodal function cannot fit the soil-water characteristic curve data for the mixtures due to the existence of two air-entry suction values for the mixtures. These values can be attributed to the existence of two distinct pore-size distributions that desaturate at different suction values.

The fits of the bimodal Brooks-Corey, van Genuchten, and Fredlund-Xing soil-water characteristic curve functions to the measured soil-water characteristic curve data for all the mixtures are shown in Figs. 6, 7, and 8, respectively. In addition, the bimodal curve fits for the pelletized diatomaceous earth from Burger and Shackelford (2001) and the unimodal curve fits for the sand used in the mixture from Fig. 4 also are shown in Figs. 6–8 for comparison. The bimodal curve fit parameters resulting from fitting the measured data for the mixtures with the bimodal Brooks-Corey, van Genuchten, and Fredlund-Xing functions are listed in Tables 6, 7, and 8, respectively.

As shown in Figs. 6–8, the soil-water characteristic curves for the mixtures are all intermediate between those for the constituent materials used in the mixtures. Also, the shapes of the soil-water characteristic curves for the mixtures represent gradual transitions from the unimodal curve for 100% sand to the bimodal curve for 100% diatomaceous as the amount of diatomaceous earth in the mixture increases. Therefore, the soil-water characteristic curves for the sand–diatomaceous earth mixtures measured in this study are consistent with those for the individual constituent materials used in the mixtures.

The microscopic portions of the soil-water characteristic curves of the mixtures indicate a broad range in pore sizes contributing to the microscopic porosity of the mixtures. This broad range of pore sizes is reflected by the wide range in suction values (100 kPa < ψ < 100,000 kPa) associated with

TABLE 7. Van Genuchten Bimodal Curve-Fit Parameters for Mixtures of Sand (20-60 and 10-20) and Diatomaceous Earth (CG1 and CG2)[a]

		Macroporosity Portion					Microporosity Portion				
Mixture	DE[b] (%)	θ_j (%)	θ_s (%)	α	β	R^{2c}	θ_r (%)	θ_j (%)	α'	β'	R^{2c}
CG1 and 20-60 sand	4.1	5.8	48.0	8.08	3.490	0.99	0.0	5.8	0.01	2.355	0.97
	8.7	8.8	50.0	8.87	3.310	0.99	0.0	8.8	0.01	2.454	0.98
	14.1	12.0	54.0	10.25	3.010	0.99	0.0	12.0	0.01	2.427	0.98
	27.6	18.6	61.0	12.76	2.690	0.99	0.0	18.6	0.04	1.863	0.99
CG2 and 20-60 sand	4.4	5.8	47.0	8.85	3.310	0.99	0.0	5.8	0.09	1.409	0.99
	9.4	9.0	49.0	10.36	3.050	0.99	0.0	9.0	0.05	1.604	0.96
	15.2	12.1	52.0	8.95	3.080	0.99	0.0	12.1	0.07	1.637	0.95
	29.4	18.8	57.0	11.75	2.820	0.99	0.0	18.8	0.04	1.950	0.99
CG2 and 10-20 sand	3.6	3.2	41.0	21.75	2.700	0.99	0.0	3.2	0.02	2.226	0.98
	7.8	6.5	43.0	18.69	2.830	0.99	0.0	6.5	0.12	1.451	0.96
	12.7	9.2	48.0	30.49	2.390	0.99	0.0	9.2	0.06	1.779	0.99
	25.3	15.8	54.0	20.83	2.400	0.99	0.0	15.8	0.09	1.827	0.99

[a]See Table 4.
[b]% DE = percentage of diatomaceous earth by dry weight in mixture.
[c]R^2 = coefficient of determination for curve fit.

TABLE 8. Fredlund-Xing Bimodal Curve-Fit Parameters for Mixtures of Sand (20-60 and 10-20) and Diatomaceous Earth (CG1 and CG2)[a]

		Macroporosity Portion							Microporosity Portion						
Materials	DE[b] (%)	θ_r (%)	θ_s (%)	a (kPa)	n	m	ψ_r (kPa)	Error[c]	θ_r' (%)	θ_j (%)	a' (kPa)	n'	m'	ψ_r' (kPa)	Error[c]
CG1 and 20-60 sand	4.1	7.0	48.0	0.97	23	0.46	1.5	<0.01	0.1	6.2	2500	0.93	3.78	8122	0.04
	8.7	8.8	50.0	0.92	10	0.52	1.9	<0.01	0.0	8.9	2500	1.65	6.44	3181	0.02
	14.1	12.5	54.0	0.87	14	0.39	2.0	<0.01	0.1	13.0	2500	0.88	5.42	4924	0.03
	27.6	20.6	61.0	0.75	26	0.26	1.6	<0.01	0.1	18.8	2198	1.22	6.05	3124	0.01
CG2 and 20-60 sand	4.4	5.7	47.0	0.93	10	0.62	2.0	<0.01	0.4	6.3	548	0.76	2.30	5764	0.00
	9.4	9.7	49.0	0.85	10	0.49	1.7	<0.01	0.7	9.6	407	1.09	1.92	2844	0.03
	15.2	13.7	52.0	0.91	14	0.38	1.5	<0.01	0.7	12.9	415	1.03	2.40	2167	0.06
	29.4	20.7	57.0	0.87	30	0.23	1.7	<0.01	0.2	19.2	663	1.30	3.11	1981	0.02
CG2 and 10-20 sand	3.6	4.3	41.0	0.42	7	0.75	0.8	<0.01	0.0	3.3	1102	1.23	3.74	2808	0.02
	7.8	7.6	43.0	0.45	10	0.53	0.9	<0.01	1.1	6.9	124	1.09	1.16	1772	0.05
	12.7	11.0	48.0	0.36	10	0.44	0.9	<0.01	0.7	9.4	234	1.49	1.55	1771	0.02
	25.3	18.2	54.0	0.41	11	0.31	1.2	<0.01	0.9	16.4	188	1.46	1.74	934	<0.01

[a]See Table 4.
[b]% DE = percentage of diatomaceous earth by dry weight in mixture.
[c]Error = sum of squared residuals for curve fit.

TABLE 9. Total, Microscopic, and Macroscopic Porosity Values for Mixtures of Sand (20-60 and 10-20) and Diatomaceous Earth (CG1 and CG2)

Materials	DE[a] (%)	Total porosity, n_T	Soil-water characteristic curve function	Microscopic porosity, n_m	Macroscopic porosity, n_M
CG1 and 20-60 sand	4.1	0.477	Brooks-Corey	0.057	0.420
			van Genuchten	0.058	0.419
			Fredlund-Xing	0.062	0.415
			Average	0.059	0.418
	8.7	0.503	Brooks-Corey	0.088	0.415
			van Genuchten	0.088	0.415
			Fredlund-Xing	0.089	0.414
			Average	0.088	0.415
	14.1	0.535	Brooks-Corey	0.120	0.415
			van Genuchten	0.120	0.415
			Fredlund-Xing	0.130	0.405
			Average	0.123	0.412
	27.6	0.606	Brooks-Corey	0.185	0.421
			van Genuchten	0.186	0.420
			Fredlund-Xing	0.188	0.418
			Average	0.186	0.420
CG2 and 20-60 sand	4.4	0.472	Brooks-Corey	0.056	0.416
			van Genuchten	0.058	0.414
			Fredlund-Xing	0.063	0.409
			Average	0.059	0.413
	9.4	0.491	Brooks-Corey	0.090	0.401
			van Genuchten	0.090	0.401
			Fredlund-Xing	0.096	0.395
			Average	0.092	0.399
	15.2	0.518	Brooks-Corey	0.118	0.400
			van Genuchten	0.121	0.397
			Fredlund-Xing	0.129	0.389
			Average	0.123	0.395
	29.4	0.571	Brooks-Corey	0.186	0.385
			van Genuchten	0.188	0.383
			Fredlund-Xing	0.192	0.379
			Average	0.189	0.382
CG2 and 10-20 sand	3.6	0.406	Brooks-Corey	0.032	0.374
			van Genuchten	0.032	0.374
			Fredlund-Xing	0.033	0.373
			Average	0.032	0.374
	7.8	0.431	Brooks-Corey	0.064	0.367
			van Genuchten	0.065	0.366
			Fredlund-Xing	0.069	0.362
			Average	0.066	0.365
	12.7	0.478	Brooks-Corey	0.090	0.388
			van Genuchten	0.092	0.386
			Fredlund-Xing	0.094	0.384
			Average	0.092	0.386
	25.3	0.545	Brooks-Corey	0.152	0.393
			van Genuchten	0.158	0.387
			Fredlund-Xing	0.164	0.381
			Average	0.158	0.387

[a]% DE = percentage of diatomaceous earth by dry weight in mixture.

decreases in volumetric water content below the volumetric water content associated with the microscopic air-entry suction (Figs. 6–8). A broad range in pore sizes also is indicated by low λ' values for the bimodal Brooks-Corey fit (Table 6).

Microscopic and Macroscopic Porosity

Following the procedure used by Burger and Shackelford (2001), the portion of the total porosity of the mixture attributable to the microscopic porosity, n_m, due to the existence of the diatomaceous earth in the mixtures is assumed to be equal to the junction volumetric water content, θ_j, regressed from the bimodal soil-water characteristic curve data when all the micropores are saturated (that is, $n_m = \theta_j$). The macroscopic porosity, n_M, then is calculated as the total porosity minus the microscopic porosity (that is, $n_M = n_T - n_m$), based on the minimum total porosity values in Table 1. The resulting values of total porosity (n_T), microscopic porosity (n_m), and macroscopic porosity (n_M) based on each of the three bimodal soil-water characteristic curve fits for n_m are listed in Table 9 for the sand–diatomaceous earth mixtures. The results in Table 9 indicate that there is little difference in the n_m values determined using the different functions, although the bimodal Fredlund-Xing function predicts slightly higher microscopic porosities relative to the bimodal Brooks-Corey and van Genuchten functions.

DISCUSSION

Dual Porosity of Mixtures

Burger and Shackelford (2001) reported average values for the total, microscopic (intrapellet), and macroscopic (interpellet) porosities of 0.764, 0.344, and 0.420, respectively, for specimens containing only CG1 pellets, and 0.725, 0.348, and 0.377, respectively, for specimens containing only CG2 when the specimens were tested at the maximum dry density. The approximately equal microscopic porosity values of 0.344 and 0.348 for the CG1 and CG2 pellets, respectively, were attributed to the existence of similar internal pore structures for the

two diatomaceous earth materials. The greater macroscopic porosity of CG1 relative to CG2 was attributed to the slightly smaller pellet sizes of CG1 (Fig. 2), since macroscopic porosity values are lower for materials with larger particle sizes. Burger and Shackelford (2001) also noted that their estimates of the percentage of the total porosity that could be attributed to the microscopic porosity compared very well with previously reported estimates based on the results of tests performed using mercury intrusion porosimetry.

In contrast to the results for the two diatomaceous earth materials reported by Burger and Shackelford (2001), the soil-water characteristic curve data for the sands used in this study were fit with unimodal soil-water characteristic curve functions reflecting the existence of only one pore-size distribution. Thus, as expected, the soil-water characteristic curves for the sands do not reflect the existence of a microscopic (intragranular) porosity region.

Therefore, based on consideration of the soil-water characteristic curves for the constituent materials used in the sand–diatomaceous earth mixtures evaluated in this study, the bimodal shapes of the soil-water characteristic curves for the mixtures can be attributed to the existence of two pore-size distributions resulting from the diatomaceous earth content. The first pore-size distribution corresponds to the soil-water characteristic curve data in the relatively low soil suction range (for example, $\psi < 100$ kPa) and is associated with pore water trapped between the larger, intergranular pores between the sand particles and the diatomaceous earth pellets. This pore-size distribution corresponds to the macroscopic porosity region for the mixture. The second pore-size distribution corresponds to the soil-water characteristic curve data in the relatively high soil suction range (for example, $\psi > 1{,}000$ kPa) and is associated with pore water that is trapped within the smaller, intraaggregate (intrapellet) pores existing entirely within the domain of the individual diatomaceous earth pellets. This pore-size distribution corresponds to the macroscopic porosity region for the mixture.

As shown in Fig. 9, the total and microscopic porosity of the mixtures increases with increased diatomaceous earth content, as expected. However, the macroscopic porosity does not change significantly for mixtures with the same constituent materials but different percentages of diatomaceous earth. The independence of the macroscopic porosity of the mixtures from the diatomaceous earth content is consistent with the similarity between the sizes of the sand grains and the diatomaceous earth pellets in the mixtures, as shown in Fig. 2.

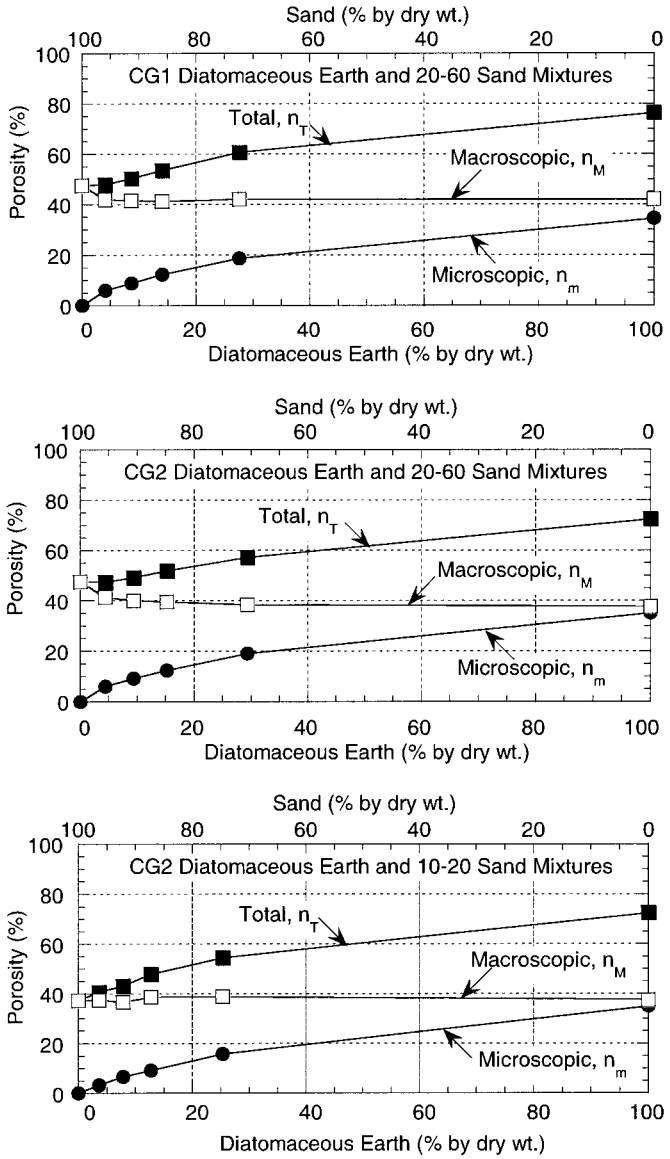

FIG. 9. Average Values for Total, Microscopic, and Macroscopic Porosity of Sand–Diatomaceous Earth Mixtures as Function of Diatomaceous Earth Content in Mixture

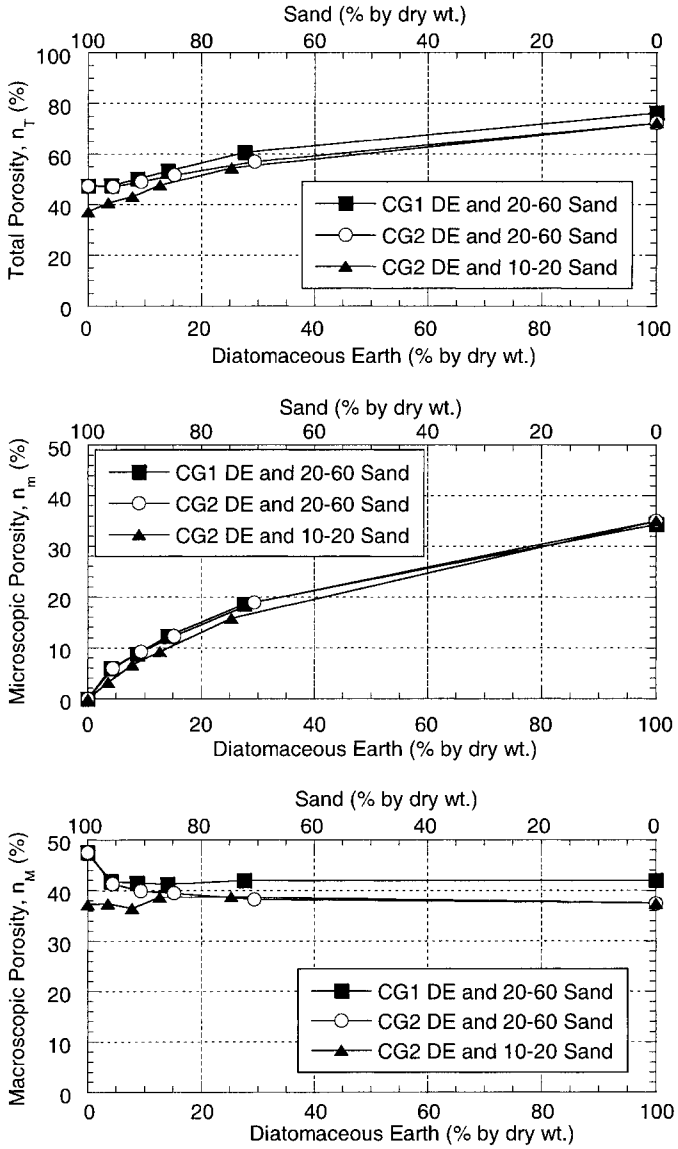

FIG. 10. Effect of Mixture Constituent Materials on Average Values for Total, Microscopic, and Macroscopic Porosity of Sand–Diatomaceous Earth Mixtures

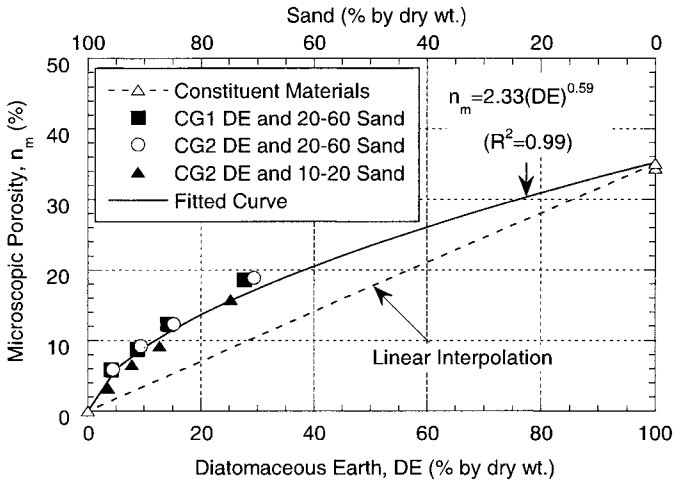

FIG. 11. Effect of Diatomaceous Earth Content on Average Value for Microscopic Porosity Considering All Sand–Diatomaceous Earth Mixtures

Comparison of Soil-Water Characteristic Curves of Mixtures

As shown in Figs. 6–8, desaturation of the microscopic porosity of the sand–diatomaceous earth mixtures begins at approximately the same suction value, regardless of the percentage of diatomaceous earth. This apparent independence of the suction at which desaturation of the microscopic (intrapellet) porosity occurs is expected on the basis of the similarity in the microscopic porosities of the CG1 and CG2 pellets.

The bimodal shape of the soil-water characteristic curve is better defined for mixtures with a greater percentage by dry weight of diatomaceous earth, as a result of the increased porosity associated with the microscopic pore-size distribution of the diatomaceous earth pellets. Also, the microscopic portions of the soil-water characteristic curves for mixtures that contained approximately the same percentage of diatomaceous earth are essentially independent of the type of constituent materials used in the mixtures. This observation is reflected by the closeness among the trends in microscopic porosity versus diatomaceous earth shown in Fig. 10 for the three different sets of constituent materials used in the mixtures.

However, as reflected by the macroscopic porosity data shown in Fig. 10, the type of constituent materials used in the mixture did affect slightly the macroscopic portion of the soil-water characteristic curves, particularly for diatomaceous earth contents less than 20%. The mixtures consisting of CG2 pellets and 10-20 sand tend to have slightly lower air-entry suctions than the mixtures consisting of CG1 and CG2 pellets and 20-60 sand. Since larger particle sizes are expected to result in larger pore sizes and lower air-entry suctions, this observation is consistent with the larger pellet sizes associated with CG2 relative to CG1, and the larger grain sizes of the 10-20 sand relative to the 20-60 sand, as shown in Fig. 2.

Estimating Microscopic Porosity of Sand–Diatomaceous Earth Mixtures

The percentage of diatomaceous earth by dry weight versus the microscopic porosity based on the average values obtained from fitting all three functions to the measured soil-water characteristic curve data (Table 9) for all the mixtures is shown in Fig. 11. The microscopic porosity of the mixtures increases nonlinearly as the percentage of diatomaceous earth in the mixture increases. As shown in Fig. 11, a simple function of the form $y = ax^b$ with $a = 2.33$ and $b = 0.59$ fits all of the data with a coefficient of determination (R^2) of 0.99. Thus, a simple linear interpolation based on the percentage of the diatomaceous earth in the mixture and the limiting microscopic porosity for the constituent diatomaceous earth underestimates the microscopic porosity of the mixture.

CONCLUSIONS

Mixtures of a relatively uniform sand with relatively similarly sized pellets of diatomaceous earth resulted in bimodal soil-water characteristic curves due to the two distinct pore-size distributions associated with microscopic and macroscopic porosity regions of the diatomaceous earth pellets. The bimodal soil-water characteristic curves of the sand–diatomaceous earth mixtures also were intermediate between the unimodal soil-water characteristic curve for the sand and the bimodal soil-water characteristic curve for the pelletized diatomaceous earth.

The method used in this study to fit bimodal soil-water characteristic curve data with the bimodal Brooks-Corey, van Genuchten, and Fredlund-Xing functions resulted in good fits of the measured data in all cases. However, the bimodal Brooks-Corey function did not fit the measured data near the air-entry suction for the microscopic porosity as well as the bimodal van Genuchten and Fredlund-Xing functions, due to the discontinuity at the air-entry suction in the Brooks-Corey function. The bimodal van Genuchten function visually fit the data the best. The bimodal Fredlund-Xing function also matched the data well, but contains eight fitting parameters, as opposed to four fitting parameters for the bimodal Brooks-Corey and van Genuchten functions.

Values for the microscopic and macroscopic porosity of the mixtures were obtained from the curve fits. For a given set of mixture-constituent materials, the total porosity of the mixtures increased from ~40 to ~75%, and the microscopic porosity increased from 0 to ~35%, as the percentage by dry weight of diatomaceous earth in the mixture increased from 0 to 100%. However, the macroscopic porosity of the mixtures was relatively constant and therefore independent of the diatomaceous earth content for all mixtures, due to the similarity in the particle sizes of the sands and diatomaceous earth pellets used in the mixtures. Thus, the differences in the soil-water characteristic curves of the mixtures result from the increase in the microscopic porosity that occurs with an increase in the percentage by dry weight of diatomaceous earth in the mixture.

REFERENCES

Breese, R. O. Y. (1994). "Diatomite." *Industrial minerals and rocks*, 6th Ed., Vol. 1, Society for Mining, Metallurgy, and Exploration, Littleton, Colo., 397–412.

Brooks, R. H., and Corey, A. T. (1964). "Hydraulic properties of porous media." *Hydro. Paper No. 3*, Civ. Engrg. Dept., Colorado State University, Fort Collins, Colo.

Burger, C. A., and Shackelford, C. D. (2001). "Evaluating dual porosity of pelletized diatomaceous earth using bimodal soil-water characteristic curve functions." *Can. Geotech. J.*, 38(1), 53–66.

Capik, M. L., and Khilnani, K. (1989). "Diatomaceous soils: A new approach." *Civ. Engrg.*, ASCE, 59(2), 68–70.

Day, R. W. (1995). "Engineering properties of diatomaceous fill." *J. Geotech. Engrg.*, ASCE, 121(12), 908–910.

Fredlund, D. G., and Xing, A. (1994). "Equations for the soil-water characteristic curve." *Can. Geotech. J.*, 31(4), 521–532.

Fredlund, M. D., Fredlund, D. G., and Wilson, G. W. (2000). "An equation to represent grain-size distribution." *Can. Geotech. J.*, 37(4), 817–827.

Leong, E. C., and Rahardjo, H. (1997). "Review of soil-water characteristic curve equations." *J. Geotech. and Geoenvir. Engrg.*, ASCE, 123(12), 1106–1117.

Smettem, K. R. J., and Kirby, C. (1990). ''Measuring hydraulic properties of stable aggregated soil.'' *J. Hydro.*, 117(1–4), 1–13.
Stoicescu, J. T., Haug, M. D., and Fredlund, D. G. (1998). ''The soil-water characteristics of sand-bentonite mixtures used for liners and covers.'' *Proc., 2nd Int. Conf. on Unsaturated Soils*, International Academic Publishers, Beijing, Vol. 1, 143–148.
Sundine Enterprises. (1996). *Isolite product literature*, Arvada, Colo.
van Genuchten, M. T. (1980). ''Closed-form equation for predicting hydraulic conductivity of unsaturated soils.'' *Soil Sci. Am. J.*, 44(5), 92–898.
van Genuchten, M. T., Leij, F. J., and Yates, S. R. (1991). ''RETC code for quantifying hydraulic functions of soils.'' *EPA Rep. 600/2-91/065*, U.S. Salinity Lab., Agr. Res. Service, U.S. Department of Agriculture, Riverside, Calif.